ELSEVIER

Journal of Applied Geophysics 33 (1995) 7–14

APPLIED GEOPHYSICS

Ground penetrating synthetic pulse radar: dynamic range and modes of operation

S.-E. Hamran, D.T. Gjessing, J. Hjelmstad, E. Aarholt

Environmental Surveillance Technology Programme (PFM), PO Box 89, 2001 Lillestrøm, Norway

Received 12 December 1992; accepted 25 November 1993

Abstract

The dominant parameter characterizing a ground penetrating radar (GPR) system is its dynamic range. The dynamic range is indicative of the penetration potential of a given system. It is the purpose of this paper to give an outline of how the dynamic range of radar systems can be calculated and compared. This is done using the radar equation coupled with the concept of a matched filter receiver. The dynamic range of an impulse radar is compared with the dynamic range of a synthetic pulse radar. The conclusion is that a synthetic pulse radar system developed by the authors' organisation has a 40 dB higher dynamic range than that of a commercially available GPR system. The potential dynamic range of the synthetic pulse GPR system is more than 200 dB.

1. Introduction

To obtain range resolution in a radar system a certain bandwidth is needed. The range resolution, ΔR, is then approximately given by the basic equation:

$$\Delta R = \frac{c}{2\Delta f} \tag{1}$$

where Δf is the bandwidth of the transmitted spectrum and c the phase velocity. Many different waveforms can be used to generate the needed bandwidth/range resolution. Three commonly used techniques are time compression (spread spectrum modulation), real pulse, and synthetic pulse. For more detailed discussions on waveforms the reader may refer to Ulaby et al. (1982) and Wehner (1987). For a survey of different radar techniques used in subsurface radar the reader may refer to Daniels et al. (1988).

In the time compression technique a long time/phase coded pulse train is transmitted. The received signal is compressed by correlation with a stored reference of the code or by matched-filter processing (Wehner, 1987). A phase coded GPR system has been developed for GPR use (Nicollin et al., 1992). The most direct GPR technique is one in which a real pulse is transmitted and the scattered energy received as a function of time. The impulse radar employs a short DC-pulse fed to an antenna (transducer), the pulse is bandpass-filtered as a result of the bandwidth of the antenna, and the shape of the pulse is determined by the transfer function of the antenna. This way of generating a pulse usually generates undesirable ringing in the time domain and thus limits the dynamic range of the radar observations. Another widely used pulse technique in ice probing radars is to time-gate a CW signal. The bandwidth/range resolution of this technique is determined by the pulse length.

A third technique is to measure in the frequency domain directly and use inversion techniques to obtain the time function in physical space. This is known as

SSDI 0926-9851(94)00026-K

the synthetic pulse method and different implementation schemes are possible. These may include direct discrete sampling in the frequency domain as well as combined time/frequency modulation schemes. The synthetic pulse technique was first described by Ruttenberg and Cahnzit (1968), and has been widely used in laboratory measurements of radar cross-section measurements. This technique has also been used in subsurface radar systems (Robinson et al., 1974; Iizuka et al., 1984; Uratsuka et al., 1988; Ødegård et al., 1992; Hamran and Aarholt, 1993).

There are different waveforms in use in current GPR applications. When deciding what waveform to use, different factors must be considered such as: flexibility, weight, price, complexity and dynamic range. In this paper only the latter aspect will be discussed.

It is useful to have a numerical factor for quantifying the sensitivity or performance of a radar system. This factor, here called the dynamic range of the radar, is defined as the maximum loss the transmitted radar signal can sustain and still be detectable at the receiver. This factor can be used for comparing different systems and when computing the potential penetration range of a system. The discussion here will be based on the radar equation coupled with the use of a matched filter receiver.

2. Matched receiver

It is known from detection theory that the maximum signal- to-noise ratio is obtained when the radar receiving system is matched to the received signal. Normally the matched filter is designed to match the transmitted signal. However modern techniques also takes the scattering target object into account (Gjessing, 1986). The maximum theoretical signal-to-noise ratio is (DiFranco and Rubin, 1968):

$$\left(\frac{S}{N}\right)=\frac{2E_R}{N_0} \tag{2}$$

where E_R is the energy of the received signal and $N_0/2$ the spectral density of the background noise. The transmitted signal energy E_T for a source signal of power $P_T(t)$ and duration τ is:

$$E_T=\int_0^{\tau} P_T(t)\,dt \tag{3}$$

The received signal energy, E_R, at a given time τ_0 relative to the transmitted signal is given by:

$$E_R=\int_{\tau_0}^{\tau_0+\tau} P_R(t)\,dt \tag{4}$$

where P_R is the received power given by the radar equation as discussed later. The signal-to-noise ratio is independent of the signal waveform and only dependent on the signal energy and the noise spectral density. This is true provided that the receiver is matched to the signal. If the receiver is not optimally matched, a reduction in signal-to-noise ratio called the filter mismatch loss has to be taken into account.

3. The radar equation

The radar equation modified to take into account attenuation in the propagation medium is

$$P_R=\frac{P_T G_T G_R \lambda^2 \sigma e^{-2\alpha R}}{(4\pi)^3 R^4} \tag{5}$$

where P_R is the received power; P_T is the transmitted power; G_T is the transmitter antenna gain; G_R is the receiver antenna gain (in this analysis assume $G_T=G$); λ is the wavelength in the medium; σ is the radar scattering cross section of the object; α is the attenuation coefficient of the medium; and R is the range to the scattering object.

For a more detailed description of the different parameters involved, the reader may refer to DiFranco and Rubin (1968), Ulaby et al. (1982), and Wehner (1987).

Combining Eqs. (1–4) yields the system signal-to-noise ratio:

$$\left(\frac{S}{N}\right)=\frac{E_T G^2 \lambda^2 \sigma e^{-2\alpha R}}{(4\pi)^3 R^4 (N_0/2)} \tag{6}$$

The power spectral density depends on the noise characteristics of the radar receiver and antenna, and is given by:

$$(N_0/2)=k_B T_0 F_N \tag{7}$$

where k_B is the Boltzman constant (1.38×10^{-23} J/K); T_0 is the system temperature (290 K); and F_N is the system noise factor.

If the receiver is not matched, a loss must be introduced. Several factors are involved in this loss and are taken into account by the matching coefficient C_M (= 1 if matched). Eq. (6) then becomes:

$$\left(\frac{S}{N}\right)=\left[\frac{E_T C_M G^2}{k_B T_0 F_N}\right]\cdot\left[\frac{\lambda^2\sigma e^{-2\alpha R}}{(4\pi)^3 R^4}\right] \tag{8}$$

In the above equation, the two factors respectively refer to the radar system dependent parameters and to the medium dependent parameters.

The signal-to-noise ratio is directly proportional to the transmitted energy. Thus, the longer the receiver integration time, the higher the signal-to-noise-ratio will be. The average transmitting power over a time period τ_i is given by:

$$\hat{P}_T=\frac{E_T}{\tau_i} \tag{9}$$

Using this relation in the first factor of Eq. (6) the dynamic range, DR, of the radar system is:

$$DR=\frac{\hat{P}_T \tau_i C_M G^2}{k_B T_0 F_N} \tag{10}$$

This factor can be used when calculating penetration depths for a given radar system for different subsurface conditions.

When comparing different radar systems, the same integration time should be used. In the following analysis, the integration time is selected to be 1 s. If in the practical system this is not the case, the results may be modified in direct proportion to the actual system integration time. Comparing two radar systems with the same antennas and integration time, the following expression is obtained:

$$\frac{\left(\frac{S}{N}\right)_1}{\left(\frac{S}{N}\right)_2}=\frac{\frac{\hat{P}_{T1} C_{M1}}{F_{N1}}}{\frac{\hat{P}_{T2} C_{M2}}{F_{N2}}} \tag{11}$$

Thus, when comparing different radar systems only the transmitted average power, receiver noise figure and the receiver matching coefficient must be considered. The dynamic range given by Eq. (10) expresses the maximum loss that the radar system can overcome. Another factor entering the discussion is the receiver dynamic range. This factor is normally given by the bit resolution provided by the receiver A/D-converter. The dynamic range of the receiver is an indication of the maximum difference that may exist between a strong reflector and a weaker one.

4. Real pulse system

A real pulse radar system transmits a pulse of length, τ, peak power, P_T, and repetition frequency $f_r = 1/\tau_r$. The average transmitted power is:

$$\hat{P}_T = f_r P_T \tau \tag{12}$$

Various receivers are in use in commercially available radar systems. First a modern receiver using digital storage will be considered. If a flash A/D-conversion technique is used in which all range cells from each transmitted pulse are simultaneously sampled as shown in Fig. 1 and coherent integration is performed in the receiver, the receiver is closely matched to the transmitted signal and $C_M \approx 1$. However, many GPR systems use repetitive transient sampling (sampling-oscilloscope technology) where single successive samples are taken for each repeated transmitted pulse as shown in Fig. 1. In this case, the receiver is not matched and the factor C_M must be modified to:

$$C_M=\frac{1}{n_p} \tag{13}$$

where n_p is the number of transmitter pulses needed to build one receiver output trace recording. The practical bandwidth of flash A/D's available today is in the order of 20 MHz whereas the repetitive transient time-domain sampling process may typically have a bandwidth in excess of 1 GHz. Thus, if a high-resolution radar is needed a system employing time-domain repetitive transient sampling must be used.

In this discussion, the receiver bandwidth of the system is assumed to be the inverse of the pulse length τ. This is necessary for the receiver to be optimally matched; if not the effect must be included in C_M.

A typical commercially available high-power impulse radar has the following system parameters:

P_T = 200 W
τ = 10ns (100 MHz bandwidth)
τ_r = 1/30 kHz
n_p = 500
G = 0 dB

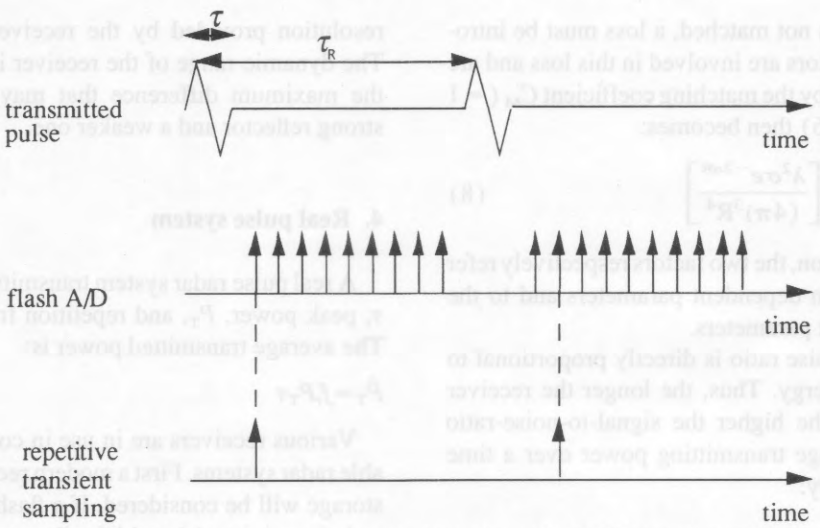

Fig. 1. An impulse radar use either repetitive transient sampling or flash A/D converters in the receiver.

$F_N = 20$
$T_0 = 290$ K

If 500 range samples are assumed to be taken per depth recording, then the system dynamic range is:

DR = 152 dB ($\tau_i = 1$ s)

If a bandwidth of 1 GHz is needed and the ambiguity range is to be kept, the dynamic range is reduced to 132 dB. This decrease stems from first a 10 dB loss in average power due to pulse length reduction (Eq. 12), and second an increased loss in the receiver mismatch (Eq. 13), in that ten times as many pulses are needed.

5. CW synthetic pulse radar system

First consider a synthetic pulse radar operating in the CW mode in which n_f frequencies are transmitted in sequence, each being $\Delta\tau$ long at power P_T. During this sequence, the radar system requires time to store the data as illustrated in Fig. 2. If the sweep repetition time is τ_r, then the average transmitted power is:

$$\hat{P}_T = P_T n_f \frac{\Delta\tau}{\tau_r} \qquad (14)$$

If the receiver bandwidth at each component frequency is $1/\Delta\tau$, then the receiver is almost matched and:

$$C_M = \frac{n_f \Delta\tau}{\tau_r} \qquad (15)$$

In a practical radar system, the change from one frequency to the next is not instantaneous and, therefore, time is needed for the synthesiser to stabilise as shown in Fig. 3. Thus, a further matching loss must be included.

A synthetic pulse radar of this type developed by the authors' organisation has the following technical data:

$P_T = 1$ W
$\Delta\tau = 1/3$ kHz
$\tau_r = 200$ ms
$n_f = 200$
$G = 0$dB
$F_N = 2$
$T_0 = 290$ K

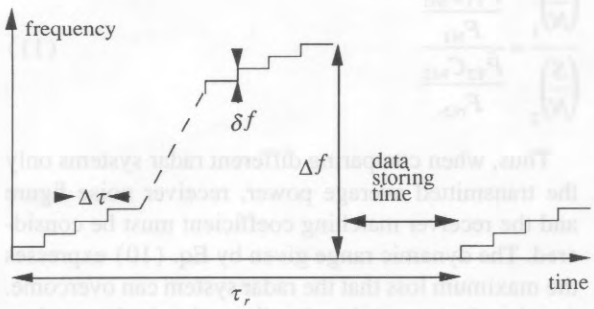

Fig. 2. The synthetic pulse radar transmits a series of CW signals.

τ_s -synthesizer transition time

τ_i -integration time

Fig. 3. In a practical frequency-stepped radar system the change from one frequency to the next is not instantaneous.

These parameters results in a dynamic range of:

DR = 191 dB (τ_i = 1 s)

The transmitted peak power in the synthetic pulse radar is 200 W after synthesizing a pulse which is the same as for the impulse radar discussed earlier. Thus the main difference between the two techniques is in the receivers. For the synthetic pulse radar, all, of the range cells are sampled all the time and, thus, the effective integration time is much longer than in the impulse system where only one range sample is taken per transmitted pulse.

The dynamic range given above is difficult to obtain in a practical system because the direct coupling between the transmitter and the receiver tends to saturate the receiver. The solution to this is to reduce the direct signal by range gating the system.

6. Range gated synthetic pulse radar

The parameters ultimately limiting the dynamic range of the radar system are the transmitting power, the antenna gain, and the system thermal noise. The thermal noise floor is determined by the receiver noise figure and the integration time/bandwidth for each frequency. It will be shown that the spatial resolution in a synthetic pulse system is not dependent upon the noise floor as in many pulsed radar systems.

The dynamic range of the receiver is limited by the resolution of the quadrature detector. If the quadrature detector is digital, the number of bits in the A/D-converter determines the dynamic range. In processing the data from the frequency domain to the time domain, a FFT can be used. This inversion generates the well-known sidelobes associated with the limited bandwidth in the frequency domain. Depending upon the window function used, sidelobes with decreasing strength will appear in the delayed reconstructed reflected signal. Fig. 4 shows the response from a point reflector for two different bandwidth window functions: square and Hanning. A receiver with 72 dB dynamic range (12-bit A/D-conversion) is illustrated and the thermal noise floor is indicated. It is seen that using the square window function the sidelobes limit the dynamic range of the radar system. Making use of a Hanning window reduces the resolution (wider synthetic pulse duration), but the dynamic range is increased and is limited by the quantization noise in the receiver.

Still the ultimate detection threshold limit, the thermal noise floor, is not reached. This brings forward the idea to gate the system so as to reduce the strength of

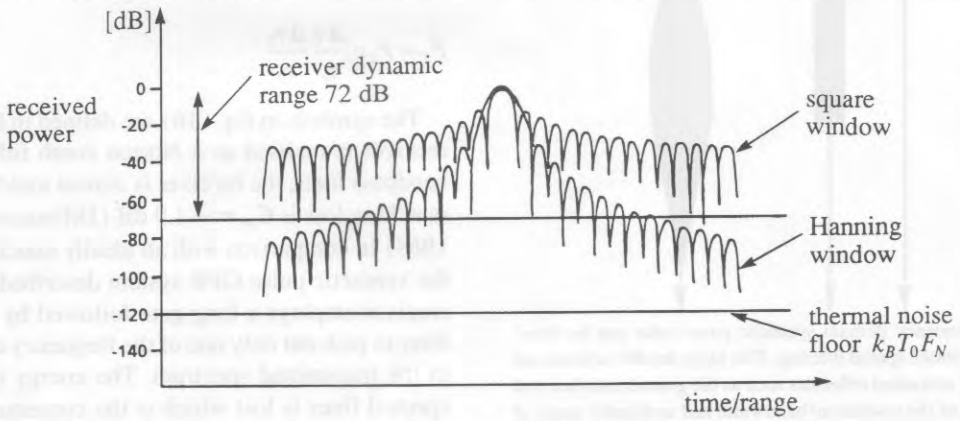

Fig. 4. Received response from a point reflector using different window functions.

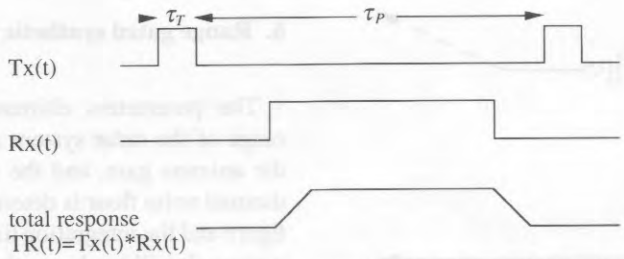

Fig. 5. The total response of the gating scheme is the convolution of the transmitted signal and the receiver gate.

strong reflections so as to make use of the total dynamic range of the system. This is achieved when the quantization noise equals the thermal noise.

Fig. 5 shows the gating scheme used. The total gating response given in Fig. 5 is the weighting effect the gating has on the medium radar response in time. Thus the amplitude weighting function on the synthesized radar range response. This response can be shown to be the convolution between the transmitter gate function and the receiver gate function. The observed response is then the multiplication between TR(t) and the backscattered energy as a function of time.

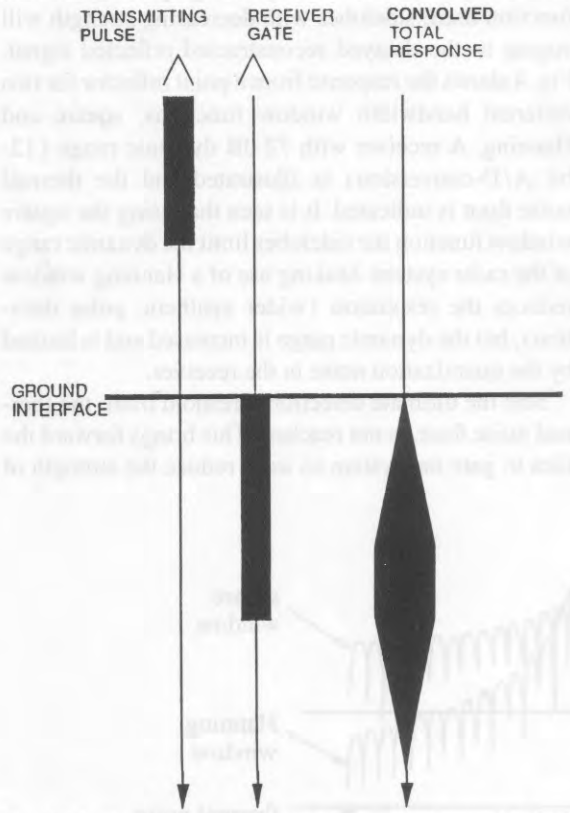

Fig. 6. The frequency domain synthetic pulse radar can be time/range gated to obtain spatial filtering. This higly flexible scheme can gate out strong unwanted reflectors such as the ground interface and is independent of the resolution/bandwidth and ambiguity range of the radar system.

Using the gate in a measuring scheme whereby the system response is stepped down in depth removing strong reflections combined with an automatic gain control in the receiver, results in a very high dynamic range in the reconstructed image. Fig. 6 shows how such gating can be used to take away the ground interface in an airborne radar system. It is worth noting that, in comparison with a real pulse radar system, the pulse sidelobes do not exist in the raw data of the synthetic pulse radar, they exist only after transformation to the time domain. It is therefore possible to remove strong reflectors very efficiently by gating. By filtering out the strong ground reflector the sidelobes in depth are also removed.

If the synthetic pulse radar is not operated CW but in the time/range gated mode discussed above, further modifications are needed in the system performance equations. When each frequency is gated, a further loss must be applied to the transmitted energy according to the duty cycle illustrated in Fig. 5:

$$\hat{P}_T = P_T n_f \frac{\Delta\tau}{\tau_r} \frac{\Delta\tau_T}{\tau_P} \tag{16}$$

The symbols in Eq. (16) are defined in Fig. 5. If the receiver is realised as a Norton comb followed by a bandpass filter, the receiver is almost matched and the matching loss is $C_M \approx -1.9$ dB (DiFranco and Rubin, 1968) in comparison with an ideally matched filter. In the synthetic pulse GPR system described earlier, the receiver employs a long gate followed by a bandpass filter to pick out only one of the frequency components in the transmitted spectrum. The energy in the other spectral lines is lost which is the consequence of not having a matched receiver. This mismatch can be

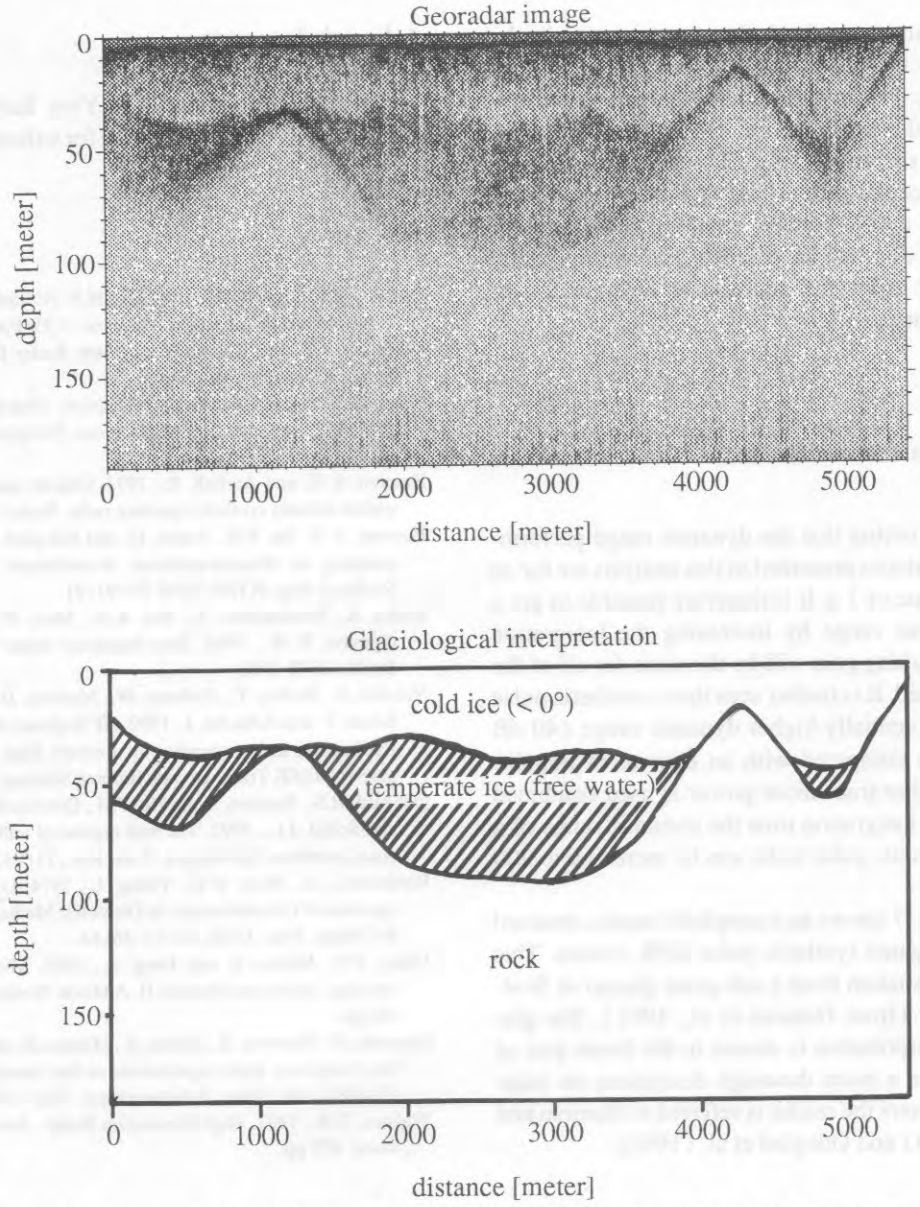

Fig. 7. The profile in the upper image was obtained using a range gated synthetic pulse radar operating in the frequency range of 320MHz to 370MHz. The lower diagram shows the glaciological interpretation. It is seen that the free water within the temperate ice gives rise to scattering [from Hamran et al, 1991].

approximately set equal to the loss of energy in the spectrum:

$$C_M = \frac{\Delta \tau_T}{\tau_P} \tag{17}$$

As seen in Eq. (3) the received energy integral is taken at a given time τ_0 corresponding to a given reflection range or depth. It is further assumed that the receiver is on during the entire time when the transmitted pulse is propagating through the range τ_0. This is always true in a real pulse radar system but not necessarily true in a range-gated synthetic pulse radar. The transmitted pulse length is not associated with the resolution of the radar and thus can be much longer.

Optimum gating is obtained when the transmitted pulse length equals the travel time to the scattering object. However, Eq. (3) is valid if the transmitted pulse is shorter than the depth τ_0, i.e. the integration is performed over the entire pulse. If the transmitter gate equals the receiver gate, a loss of 6 dB is introduced compared to a CW-system, resulting in a dynamic range of 185 dB with no practical limitations caused by feed-over from the transmitter antenna to the receiver antenna.

7. Discussion and conclusions

It is worth noting that the dynamic range performance characteristics presented in this analysis are for an integration time of 1 s. It is therefore possible to get a higher dynamic range by increasing the integration time. The resulting gain will be the same for all of the waveforms used. It is further seen that a synthetic pulse radar has a potentially higher dynamic range (40 dB higher) when compared with an equivalent impulse radar. If a higher transmitter power is used combined with a longer integration time the dynamic range of a practical synthetic pulse radar can be increased to 200 dB or higher.

Finally, Fig. 7 shows an example of results obtained with a range gated synthetic pulse GPR system. This radar profile is taken from a sub-polar glacier at Svalbard, Norway (from Hamran et al., 1991). The glaciological interpretation is shown in the lower part of the figure. For a more thorough discussion on radar studies of glaciers the reader is referred to Hamran and Aarholt (1993) and Ødegård et al. (1992).

Acknowledgements

The authors are grateful to Yves Barbin at Service d'Aeronomie, CNRS in France for valuable comments.

References

Daniels, D.J., Gunton, D.J. and Scott, H.F. (Editors), 1988. Special Issue on Subsurface Radar. IEE Proc., 135(F,4).

DiFranco, J.V. and Rubin, W.L., 1968. Radar Detection. Artech House, Dedham, MA, 654 pp.

Gjessing, D.T., 1986. Target Adaptive Matched Illumination RADAR: Principles and Applications. Peregrinus, London, 172 pp.

Hamran, S.-E. and Aarholt, E., 1993. Glacier study using wavenumber domain synthetic aperture radar. Radio Sci., 28(3).

Hamran, S.-E, Bø, P.H., Vatne, G. and Ødegård, R., 1991. Radar mapping of, Blomstrandbreen, Konsulbreen and Rantebreen, Svalbard. Rep. NTNF/PFM TN-91/91.

Iizuka, K., Freundorfer, A., Wu, K.H., Mori, H., Ogura, H. and Nguyen, V.-K., 1984. Step-frequency radar. J. Appl. Phys., 56(9): 2572–2583.

Nicollin, F., Barbin, Y., Kofman, W., Mathieu, D., Hamran, S.-E., Bauer, P. and Achache, J., 1992. HF bi-phase shift keying radar; Application to ice sounding in western Alps and Spitsbergen glaciers. IEEE Trans. Geosci. Remote Sensing, 30(5).

Ødegård, R.S., Hamran, S.-E., Bø, P.H., Etzelmuller, B., Vatne, G. and Sollid, J.L., 1992. Thermal regime of valley glacier, Erikbreen, northern Spitsbergen. Polar Res., 11(2).

Robinson, L.A., Weir, W.B., Young, L., 1974. Location and Recognition of Discontinuities in Dielectric Media Using Synthetic RF Pulses. Proc. IEEE, 62(1): 36–44.

Ulaby, F.T., Moore, R. and Fung, A., 1982. Microwave Remote Sensing, Active and Passive, II. Addison-Wesley, Reading, MA, 456 pp.

Uratsuka, S., Okamoto, K., Nishio, F., Mineno, H. and Mae, S., 1988. Step frequency radar experiments on the Antartic sea ice. Proc. IGARSS 1988 Symp., Edinburgh, pp. 1703–1706.

Wehner, D.R., 1987. High Resolution Radar. Artech House, Norwood, 472 pp.